International Journal of Energetica (IJECA)
https://www.ijeca.info
ISSN: 2543-3717 Volume 9. Issue 2. 2024 *Page 48-53*

Energetic Ionospheric Upwelling: A Case Study of Velocity Distribution and Ion Flux Observed by the EISCAT Svalbard Radar

T.W. David[1,2,*], C.M. Michael[3,2], T. D. Awoyinka[1], A.E. Ajetunmobi[1], A.T. Talabi[1]

[1]Department of Physics, Olabisi Onabanjo University, Ago-Iwoye, NIGERIA
[2]School of Physics and Astronomy, University of Leicester, Leicester, UK
[3]Faculty of Arts, Science and Technology (FAST), University of Northampton, Northampton, UK

*Corresponding author E-mail: *david.timothy@oouagoiwoye.edu.ng*

Abstract – *When outflow of heavy ions such as O+ occurs, the atmospheres of planets are gradually loss. The ions being depleted in the ionosphere, under favourable conditions, upwell into the underlying magnetosphere and forms a substantial part of plasma in the magnetosphere. The motion of the heavy ions affects the Alfvén speed as a result, alters global magnetospheric dynamics. Joule heating, electron precipitation and other suprathermal energization are part of the mechanisms involved in the outflow process. Seven hundred and sixty two 762 events of periods of noticeable velocity upflow in conjunction with activities in the electron precipitation as well as enhancement in electron and/or ion temperature(s) were observed by the EISCAT Svalbard Radar (ESR) during the 2007 campaign. The 762 events were categorized by velocity strength in a colour coded plots. A further observation of periods when the ion upward velocity covered a wide range of altitude is examined, and the distribution of the events shows that about 9.2% of the upflow velocity covers a wide range of altitude. Furthermore, analysis shows that the distribution of high velocity events (≥ 200 ms-1), in conjunction with Kp ≥ 4 is peaked around local noon while other upwelling's of moderate and low velocities with same range of Kp is skewed towards the night-side. Ion upwelling on the other hand, being a function of electron density and the corresponding velocity, shows that events of same velocity range, may belong to different flux regime, and vice versa.*

Keywords: Ionospheric upwelling, joule heating, ion flux, ion velocity, heavy ions.

Received: 09/07/2024 – Revised: 23/10/2024 – Accepted: 29/11/2024

I. Introduction

The ionospheric high latitudes contain both light thermal ions (H^+, He^+) and heavy energetic ions (e,g., O^+, O_2^+, N_2^+) [1]. Under certain conditions, oxygen ions (O^+) in the upper atmosphere can outflow into the magnetosphere, influencing magnetospheric dynamics within the sun-magnetosphere-ionosphere system. The ionosphere, a region rich in oxygen ions (O^+), experiences upwelling of heavy ions, a process that can lead to the loss of planetary atmospheres. It is believed that wave modes are responsible for accelerating these upwelling ions once they are above the atmosphere [2], though much about this acceleration process remains unclear. However, when the ambipolar electric field grows beyond a certain threshold due to increasing electron heating, there is a significant reduction in the upflowing ion flux [3].

It could also be inferred from Khazanov et al. [4] that in a collisionless space, inaccessibility regions in the velocity space could be created as particle velocity vector changes direction and magnitude as a result of changes in

either the magnetic field or the various potential energies. They explain further that in the polar cap ionosphere, the force due to the ambipolar electric field for oxygen ions (O^+) to flow out is weaker than that due to gravity. In a nut shell, suprathermal energization is required to free the upwelling heavy ions from the strong magnetic field and gravitational pull of the planet into near Earth space. Zhang et al. [5] reported two species of upwelling oxygen ion (O^+) in the polar cap region, one been energised by frictional heating, and the other by field-aligned current. Yuang et al. [6] in their analysis of Defense Meteorological Satellite Program F15 data, estimated that during intense geomagnetic storms, the polar cap boundary is rich in O^+ to support ion upwelling into the magnetosphere. Ogawa et.al. [7] in their study of ESR data in comparison with solar wind plasma parameters during solar cycle 23, observed that ion upflow variation on the dayside follows a direct relationship until the solar wind velocity reaches 650 km s^{-1}, while David et al. [8] established that upflow occurrence bears a directly relationship with an increase geomagnetic activities. Ion downflow is predominant with high solar wind speed, yet the upflow-downflow ratio will still exceed 1 [7,8]. Endo et al. [9] showed that downflow is more prevalent at midnight and though, upflow and downflow increase with an increase in *Kp* index, increase indownflow occurrence becomes negligible at higher level of *Kp*. David et al, [10] studied different categories of ion upflow with their corresponding level of associated noise, and highlighted that the noise level increases with the magnitude of the ion flux and varies seasonally.

Previous studies investigate upflows in conjunction with solar wind velocity, whereas, the analysis of the occurrence of ion upwelling identified by ion upflow velocity itself in conjunction with the *Kp* index, a measure of geomagnetic disturbance, is studied. Secondly, the upwelling is also investigated based on the ion flux strength in order to compare upwelling's caused by the same velocity regime. In comparison to previous works, a database of large set of continuous data for a complete year during the international polar year (IPY) campaign of 2007 will be studied, thereby ensuring a robust data analysis.

II. Materials and Methods

The EISCAT Svalbard Radars run on the Incoherent Scatter Radar (ISR, [11]) technique and with it, measure some basic plasma parameters of the ionosphere can be measured, these include; electron density (n_e), from the total scattered energy, ion temperature (T_i), from the spectrum width, electron temperature (T_e), from the spectrum height with a usual double hump-shaped, and the ion drift velocity (v_i). The ESR 42 m diameter fixed dish shown in Figure 1 measures the ion drift velocity along the local geomagnetic field line with a data resolution of 1 minute and it is the source of data for the electron density and ion velocity used in this work. Data for *Kp* index, a measure of geomagnetic activity, where low geomagnetic disturbance indicated by $Kp < 2$, and $2 \leq Kp < 4$, and $Kp \geq 4$ denoting medium and high disturbance respectively was also sourced for this study from the Madrigal site.

Figure 1. Fixed 42 m dish of the EISCAT Svalbard Radar. From EISCAT, 2015

III. Result and discussion

III.1. Velocity based criteria

The snapshots of the ESR parameter plots comprising the graphs of electron density, electron temperature, ion temperature, and ion drift velocity (v_i) were downloaded from the EISCAT database. By visual inspection, 762 events of periods of noticeable velocity upflow in conjunction with activities in the electron precipitation as well as enhancement in electron and/or ion temperature(s) were observed. The 762 events were categorized by velocity strength in the colour coded graphs as follows:

- Weak velocity: $50\ m\ s^{-1} \leq v_i < 100\ m\ s^{-1}$
- Fairly moderate velocity: $100\ m\ s^{-1} \leq v_i < 150\ m\ s^{-1}$
- Moderate velocity: $150\ m\ s^{-1} \leq v_i < 200\ m\ s^{-1}$
- High velocity: $200\ m\ s^{-1} \leq v_i < 300\ m\ s^{-1}$

- Very high velocity: $v_i \geq 300\ m\ s^{-1}$

Another category of upflow that is included in the observation is the period when the ion upward velocity covered a wide range of altitude. Table 1 shows the distribution of the events.

Table 1. Classification of events by velocity

Classification	Rank	Number of events
Very high	5	134 *(1)
High	4	318 *(22)
Moderate	3	170 *(17)
Fairly moderate	2	126 *(19)
Weak	1	14 *(11)
	Total	**762**

*( ): number of event(s) across wide range down to low altitude

Figure 2 shows the *Kp* distribution of events with respect to different velocity regimes. The *Kp* index is a system of numbering that scales the geomagnetic activity to indicate level of disturbed condition in the geomagnetic field. $Kp < 2$ indicates a period of low disturbance, while $2 \leq Kp < 4$ and $Kp \geq 4$ are periods of moderate and high activities respectively. Analysis shows that events with velocity regime ≥ 200 ms^{-1} (Figure 2a,b), when $Kp \geq 4$ are peaked around local noon, whereas upwelling during the same range of $Kp \geq 4$ for weak to moderate velocities is predominant from midnight till dawn (Figure 2c).

The implication of this is that high geomagnetic activities during the upwellings are predominantly related to

- high velocities events around the cusps
- moderate and low velocities events on the night side aurora

It is also worth noting that when the velocity drops below the fourth rank, events with high *Kp* no longer occur between pre-noon and noon as shown in Table 2, indicated by the red digits.

The second aspect of Figure 2 is the frequency distribution. For the very high velocity events ($\geq$ 300ms^{-1}, Figure 2a), the occurrence frequency is predominantly between pre-noon and post-noon. The ionization, being a function of the sun and activities from it, fluctuates greatly in the level to which the atmospheric constituents are being ionized. Since the solar radiation reaching the atmosphere is at a maximum around noon, it is expected that high ionization and high velocity as a result, should be peculiar to this time of the day as could been seen from graph. Seasonal variation is another effect that contributes to the variation in the ionospheric ionization; this would be investigated in another work.

The frequency distribution in Figure 2b indicates that though occurrence ionization is still dominant between the dawn and day side, frequency from both flanks are gaining momentum to level up. In Figure 2c where all categories of velocity is investigated, the dominance has moved to the night sector and early dawn. Activity from the sun continues even when solar radiation subsides, and the interaction of the activity with the geomagnetic field lines through the solar wind and the frozen-in interplanetary magnetic field (IMF) causes magnetospheric loading with energy in the nightside. At a point in time, the plasma sheet, which acts as a reservoir, has sufficient energy build-up that it becomes unstable and potential drops are generated. These potentials, according to Kivelson and Russell [12], accelerate electrons towards the Earth into the ionosphere, which collide with the atmospheric atom or molecule to cause air glow. About 52% of the events investigated are in the weak to moderate velocity regimes, and the reason it takes the lead in occurrence frequency could be due to energization of the particles from the nightside aurora, and this will be subject of further investigation

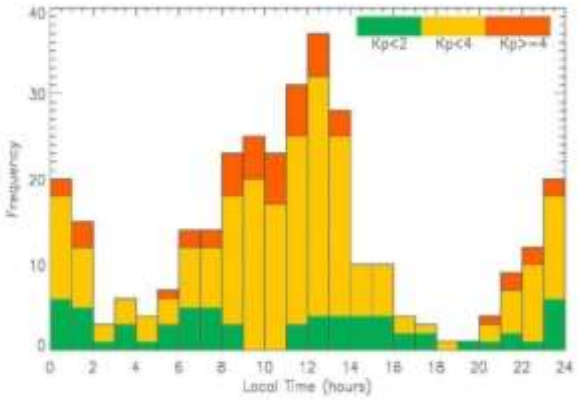

Figure 2a. *Kp* distribution of events with velocity ranked as 5

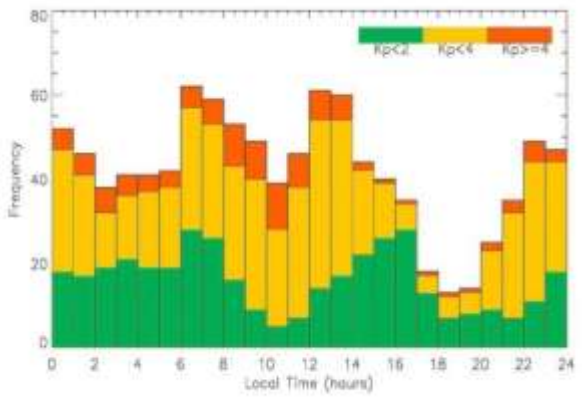

Figure 2b. *Kp* distribution of events with velocity ranked 4 and 5

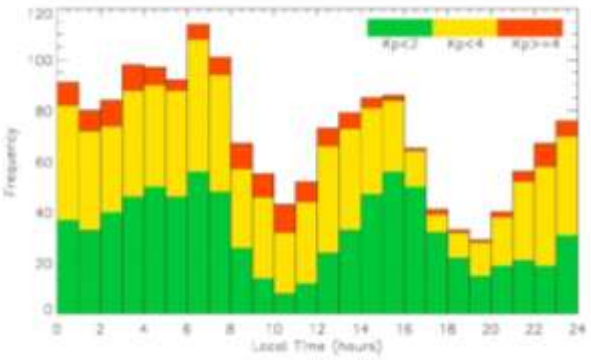

Figure 2c. *Kp* distribution of events for all ranks of velocity

Table 2. Relationship between velocity of events with high *Kp* index at different local time; indicating that events with high *Kp* no longer occur between pre-noon and noon at velocities below 200 ms^{-1}.

LT/ v_i (m/s)	0	1	2	6	7	8	9	10	11	12	13	21	22	23
>300	2	3	0	2	2	5	5	6	6	5	3	2	2	2
>200	5	5	6	5	6	10	9	11	8	7	6	3	5	3
>50	9	8	10	6	7	10	9	11	8	7	6	4	9	6

III.2. Impact of Carrier Density and Thickness of ZnS Buffer Layer on Performance Parameters

The ESR–IPY raw data is downloaded from the Madrigal website and the ion fluxes are calculated where neither the electron density nor the ion velocity is equal to $1e30$. Out of the 762 events identified by upflow velocity from the ESR snapshots, data is available for 755 events through the raw data. In order to sieve out downflows and events that are not likely to result in an upflow, a filtering technique that allows only value $\geq 1.0 \times 10^{13}\ m^{-2}\ s^{-1}$ is incorporated. About 98% of the events binned by upward velocities satisfy the $1.0 \times 10^{13}\ m^{-2}\ s^{-1}$ ion flux threshold value indicated by Wahlund et al. [13]. The fluxes that satisfied this minimum value are categorized as follows:

i. Weak: $1.0 \times 10^{13}\ m^{-2}\ s^{-1} \leq f_{ion} < 2.5 \times 10^{13}\ m^{-2}\ s^{-1}$
ii. Fairly moderate: $2.5 \times 10^{13}\ m^{-2}\ s^{-1} \leq f_{ion} < 5.0 \times 10^{13}\ m^{-2}\ s^{-1}$
iii. Moderate: $5.0 \times 10^{13}\ m^{-2}\ s^{-1} \leq f_{ion} < 7.5 \times 10^{13}\ m^{-2}\ s^{-1}$
iv. High: $7.5 \times 10^{13}\ m^{-2}\ s^{-1} \leq f_{ion} < 1.0 \times 10^{14}\ m^{-2}\ s^{-1}$
v. Very high: $f_{ion} \geq 1.0 \times 10^{14}\ m^{-2}\ s^{-1}$

The rest of this study is based on the ion flux because it gives a true picture of the upwelling ions. For example, Figure 3 compares periods of fairly moderate and high velocities with little or no difference in the ion flux.

The blue, black, orange, red and green coloured shapes represent weak, fairly moderate, moderate, high, and very high categories of flux respectively. The first panel in Figure 3 shows two events of same velocity range, but the peak flux in the first event extends to the high flux category while the second peak belongs to the moderate category. There are also two events of different velocity regimes on the same day in the second panel. The second event of the day though of velocity rank 2, has a peak flux that is greater than the first event of the day whose velocity is ranked 4. Comparison between the rank 2 and 4 velocities in the middle and bottom panels of Figure 3 respectively indicates similarity in the pattern of flux despite the difference in their class of velocity. The reason for this is because flux is the product of electron density and the corresponding velocity.

$$f_{ion} = n_e \times v_i \qquad 4.1$$

It is possible to have a period of high upflow velocity, but low density, and vice versa, which will in turn affect the ion flux.

Figure 3 further shows day-to-day variability in the ion upflow. The first panel of Figure 3 indicates ion upflow between midnight and dawn, the second panel shows dawn and noon upwellings, while prenoon and midnight upwellings are seen in the third panel. Furthermore, between the period of 4 – 6 UT, the magnitude of the ion upflows attains high flux category on day 0322, while days 0323 and 0325 indicate fairly moderate and no flux respectively between the same time interval.

Some studies in the past have sorted the ion upflows based on its velocity to categorize events, while David et al. [8] for example, based the choice of events on the flux.

The results described above from Figure 3 validates that the ion flux is a better quantity to describe upflow regime as it can be seen that different velocity regime can result in the same ion upflow and vice versa. The ion flux in the flux tube is maintained at a constant overall total unless the state is turbulent, otherwise, it is a conserved quantity. As a result, the ion flux other that its velocity should be employed when measurement of potential outflow from the ionosphere into the magnetosphere. Furthermore, the proper understanding of categorizing the heavy ion is of paramount importance as its motion affects the Alfvén speed and as a result, alters magnetospheric dynamics [14].

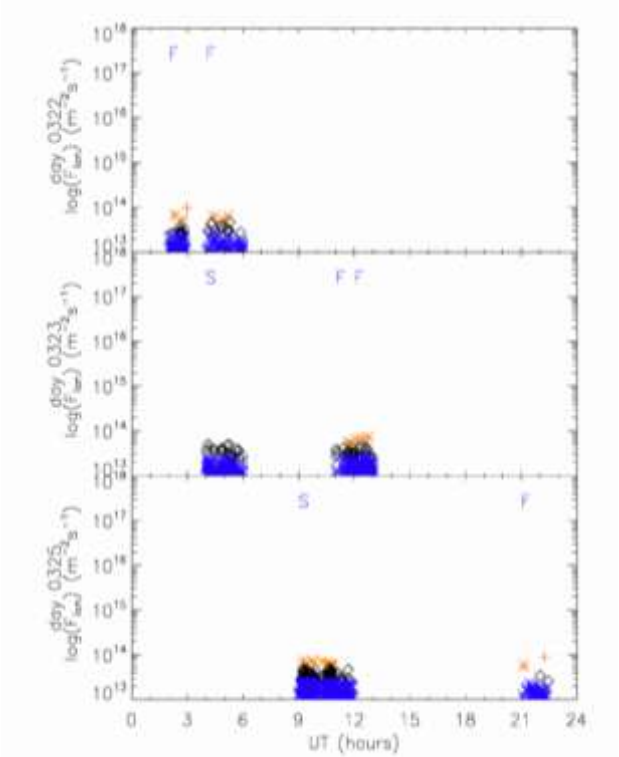

Figure 3. Comparison between velocity and ion flux: 'R2' means fairly moderate or rank 2 velocity and 'R4' means high or rank 4 velocity

IV. Conclusion

This study examined ion upwellings in the Earth's upper atmosphere during the 2007 IPY campaign, a period characterized by extremely low solar activity. Seven hundred and sixty-two (762) events were manually selected when the EISCAT Svalbard Radar (ESR) observed upflow in the ion velocity in conjunction with activities going on in the precipitation and Poynting fluxes. Ion velocity ranges between weak (rank 1) and very high (rank 5), and periods of wide coverage in altitudes are highlighted. The ion fluxes are calculated for these events and the following conclusions are arrived at:

- Analysis shows that events with velocity regime ≥ 200 ms^{-1} when geomagnetic index $Kp \geq 4$, are peaked around local noon.
- Moderate and low velocities events with $Kp \geq 4$ are predominantly skewed unto the nightside.
- Early dawn (6:00 – 7:00 UT) takes the lead in frequency distribution of events while the night sector dominates on the overall. This might be related to minimum condition in solar activity during the year 2007.
- Events with high *Kp* ceases to occur between pre-noon and noon at velocities below 200 ms^{-1}
- There are periods of low velocities driven by high densities. This condition makes the flux a better parameter over the velocity, to investigate the ion upwellings.
- Day-to day variability is observed in the ion flux.

Declaration

- The authors declare that they have no known financial or non-financial competing interests in any material discussed in this paper.
- The authors declare that this article has not been published before and is not in the process of being published in any other journal.
- The authors confirmed that the paper was free of plagiarism

Acknowledgements

The authors are deeply grateful to the EISCAT community for the data used for this work. The Olabisi Onabanjo University, Ago-Iwoye, Nigeria and University of Leicester, United Kingdom are respectively appreciated for the enabling environment provided and the software used in the analysis.

Reference

[1] Schunk, R. W. (2000). Theoretical developments on the causes of ionospheric outflow. *Journal of Atmospheric and Solar-Terrestrial Physics*, 62(2000), 399 - 420. https://doi.org/10.1016/S1364-6826(00)00017-1

[2] Hultqvist, B., Øieroset, M., Paschmann, G. and Treumann, R. (1999). *Magnetospheric plasma sources and losses (1999th ed.)*. Dordrecht, Boston, London: Kluwer Academic Publishers. https://doi.org/10.1007/978-94-011-4477-3

[3] Moore, T. E., Fok, M.-C. and Garcia-Sage, K. (2014). The ionospheric outflow feedback loop, *Journal of Atmospheric and Solar-Terrestrial Physics*, 115-116, pp. 59–66. https://doi.org/10.1016/j.jastp.2014.02.002

[4] Khazanov, G. V., Liemohn, M. W., Krivomtsky, E. N. and Moore, T. E. (1998). Generalized kinetic description of a plasma in an arbitrary field-aligned potential energy structure. *Journal of Geophysical Research*, 103(A4), 6871–6889. https://doi.org/10.1029/97JA03436

[5] Zhang, Q. H., Zong, Q. G., Lockwood, M., Heelis, R. A., Hariston, M., Jiang, J., *et al.*, (2016). Earth's ion upflow associated with polar cap patches: Global and

in situ observations. *Geophysical Research Letters*, 43, 1845–1853. https://doi.org/10.1002/2016GL067897.

[6] Yuan, Z. G., Deng, X. H. and Wang, J. F. (2008). DMSP/GPS observations of intense ion upflow in the midnight polar ionosphere associated with the SED plume during a super geomagnetic storm. *Geophysical Research Letters*, 35, L19110. https://doi.org/10.1029/2008GL035462

[7] Ogawa, Y., Buchert, S. C., Fujii, R., Nozawa, S. and van Eyken, A. P. (2009). Characteristics of ion upflow and downflow observed with the European Incoherent Scatter Svalbard radar. *Journal of Geophysical Research*, 114, A05305. https://doi.org/10.1029/2008JA013817

[8] David, T. W., Wright, D. M., Milan, S. E., Cowley, S. W. H., Davies, J. A. and McCrea, I. (2018). A study of observations of ionospheric upwelling made by the EISCAT Svalbard Radar during the international polar year campaign of 2007. *Journal of Geophysical Research-Space Physics*, 123, doi:10.1002/2017JA024802

[9] Endo, M., Fujii, R., Ogawa, Y., Buchert, S. C., Nozawa, S., Watanabe, S. and Yoshida, N. (2000). Ion upflow and downflow at the topside ionosphere observed by the EISCAT VHF radar. *Annales Geophysicae*, 18(2), 170–181. https://doi.org/10.1007/s00585-000-0170-3

[10] David, T. W., Michael, C. M., Wright, D. M., Talabi, A. T. and Ajetunmobi, A. E. (2024). Ionospheric upwelling and the level of associated noise at solar minimum. *Annales Geophysicae* 42, 349 – 354. https://doi.org/10.5194/angeo-42-349-2024

[11] Williams, P.J.S. (1995). A multi-antenna capability for the EISCAT Svalbard Radar. *Journal of Geomagnetism and Geoelectricity*, **47**, pp. 685-698. https://doi.org/10.5636/jgg.47.685

[12] Kivelson, M. G. and Russell, C. T. (1995). *Introduction to Space Physics*. First edn. United Kingdom, University of Cambridge: Cambridge University Press. https://doi.org/10.1017/9781139878296

[13] Wahlund, J. E., Opgenoorth, H. J., Haggstrom, I., Winser, K. J. and Jones, G. O. L. (1992). EISCAT observations of topside ionospheric ion outflows during auroral activity—Revisited. *Journal of Geophysical Research*, 97(A3), 3019–3037. https://doi.org/10.1029/91JA02438.

[14] Strangeway, R. J., Ergun, R. E., Su, Y. J., Carlson, C. W., & Elphic, R. C. (2005). Factors controlling ionospheric outflows as observed at intermediate altitudes. *Journal of Geophysical Research*, 110, A03221. https://doi.org/10.1029/2004JA010829